Extended Abstracts of the 17th Conference on Solid State Devices and Materials, Tokyo, 1985, pp. 393-396

B-4-6

High-Current, High-Frequency Gate Turn-Off Thyristors with P^+P^- Anode Emitter Structure

Makoto Azuma, Takashi Shinohe,
Katsuhiko Takigami and Hiromichi Ohashi

Toshiba Research and Development Center
1 Toshiba-cho, Komukai, Saiwai-ku, Kawasaki 210

High-current, high-frequency reverse blocked GTOs were developed for the purpose of application to current-mode inverters, choppers and active filters. These GTOs have a novel anode emitter structure which consists of a horizontally alternate low-high impurity concentration layer. Adopting this structure to the GTOs leads to reducing the current crowding into the central portion of the n-emitter strip during the turn-off as well as suppressing the extra carrier injection from p-emitter. As a result, the peak turn-off current increases and the switching power loss due to the tailing current decreases, thus enabling high-current, high-frequency operation.

§1. Introduction

In a high power gate turn-off thyristors (GTOs) development history of more than a decade(1)-(5), their reverse blocking capability is required in application to current-mode inverters, choppers and active filters. In these applications adopting GTOs without reverse blocking capability, such as conventional anode shorted GTOs (4)(5), needs series-connected diodes, resulting an increase in equipment weight and size due to cooling fins and several circuits. Therefore, strong requirement have been made on development of reverse blocked GTOs (RB-GTOs) with high frequency characteristics nearly equivalent to anode shorted GTOs.

From a RB-GTO design viewpoint, in general, it is necessary to reduce an n-base carrier lifetime in order to attain its higher speed operation. In more detail, the high speed characteristics can be obtained by a decrease in the tailing current flowing immediately after the turn-off, which is a major origin of power-loss in high frequency operation. The carrier lifetime reduction, however, leads to increasing the on-state voltage and the leakage current under high temperature. Accordingly, the most important subject on high-frequency RB-GTO design is to find an improving method on the trade-off relation between the high speed switching characteristic and the low on-state voltage, instead of controlling the n-base carrier lifetime.

This paper describes about effects on a low impurity doping of an anode emitter layer, a concept of novel RB-GTOs with an alternate low-high impurity doped anode emitter layer as well as their electric characteristics.

§2. Effects of a low-doped anode emitter on GTO characteristics.

In this section, we discuss effects of a low-doped anode emitter on GTO characteristics (6), which are indispensable knowledge for proceeding the discussion to the basic device structure of GTO with a low-high doped anode emitter.

Figure 1 shows impurity doping profiles of fabricated GTOs. The p-emitter diffusion was performed to prepare the three kinds of device (typeH,M,L) which

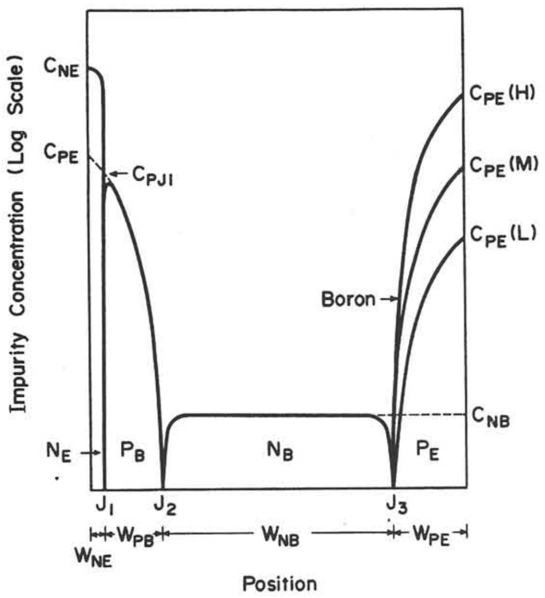

Fig.1 Impurity doping profiles of fabricated GTOs.

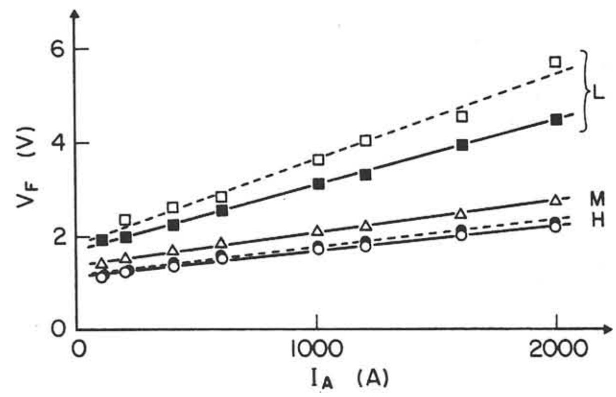

Fig.2 Anode current vs. forward voltage drop.

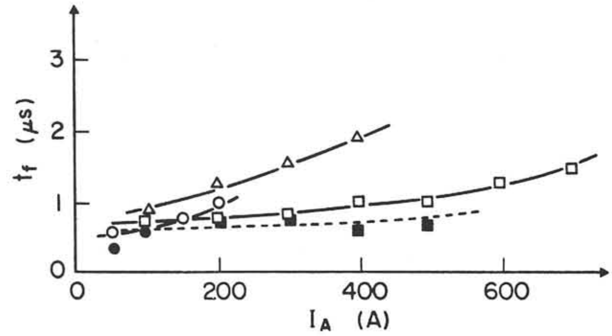

Fig.3 Anode current vs. fall time.

have the different surface impurity concentration of p-emetter (Cpe) and the same junction depth. The type M has the same Cpe as a conventional RB-GTO, and Cpe of the type H and L are 1-order higher and lower than that of the type M respectively.

Figures 2 and 3 are the anode current dependences of forward voltage drop (Vf) and fall time (tf) for the three kinds of device, respectively. As shown in those figures, the type L has different dependences from the other two types, that is to say, Vf of the type L is much larger than those of the type H and M, and tf of the type L is much smaller than those of the other two types in the all range of the anode current. And above all,it is noteworthy that the tailing current (Itl) of the type L is less than half compared with the other two types.

To examine these characteristics in more detail, we measured the current gain of the p-n-p transistor section (α pnp). As was expected from the lower injection efficiency of the type L, the type L has a lower αpnp than the other two types, from which above mentioned characteristics can be all explained by the well-known relation between αpnp and GTO characteristics.

From above results, it is confirmed that the p^--emitter GTO has the advantage of the small tailing current which allows the higher frequency operation, while it also has the large forward voltage drop which should be improved.

§3. Concept of a novel RB-GTO with a low-high doped anode emitter.

Figure 4 shows a schematic view of the fabricated GTO with a low-high doped anode emitter structure (p^+p^--emitter GTO) (7). As shown in this figure, a p-emitter layer in contact with an anode electrode is devided into two regions (p^+ and p^- regions) having different impurity concentrations, and their arrangement is corresponding to the multi n-emitter pattern. More specifically, p^- regions are formed beneath the central part of the corresponding n-emitter strips, and ring shaped p^+ regions are formed to surround the above mentioned p^- regions.

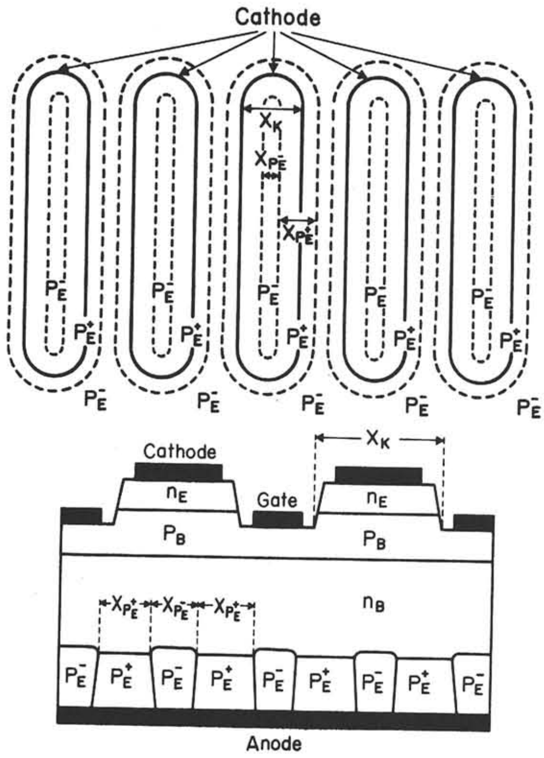

Fig.4 Schematic view of the fabricated p^+p^--emitter GTO.

As the first effect of this p-emitter structure , the current crowding into the central portion of the n-emitter strip during the turn-off (8)-(9) is suppressed and the anode current is distributed to a peripheral portion near the gate electrode to which a negative bias is applied. Thus, the anode current is easily extracted from the gate electrode, resulting an increase in I_{TGQM}.

As the second effect, the ring shaped p^+ region restricts the spread of the current path between p-emitter and n-emitter, thus suppressing the extra carrier injection from p-emitter. Therefore, the tailing current can be reduced, enabling the permissible operating frequency to be increased. Since the ring shaped p^+ region is located beneath the periphery of a pn-junction formed between n-emitter strip and p-base, where the latching current flows at the beggining of turn-on operation, small latching current can be retained.

§4. Device fabrication and characteristics.

The devies are fabricated on a 18 mm diameter silicon wafer by using a selective boron diffusion, and conventional photo masking techniques. The p-base is chemically etched down to subdivide the n-emitter strips. Gold is evaporated and diffused from the anode side to reduce the carrier lifetime for achieving fast turn-off characteristics. And their forward blocking voltage are 4500 volts.

The fabricated samples have the various Xpe^+ and Xpe^- in order to investigate the above mentioned effect of this structure. The conventional GTO with p^+-emitter is also fabricated for the comparison.

Figure 5 shows initial value of the tailing current Itl as a function of $M=(Xpe^-/2)/Xpe^+$, which is a ratio of the p^- region area to the unit GTO area, corresponding to the injection efficiency from the p-emitter. As is evident from Fig.5, Itl can be reduced to the 2/3 of the conventional RB-GTO (M=0) with an increase in the value of M. In high frequency operation (>1kHz) of high power GTOs, more than 50 percent of the total power loss is occupied by the switching power loss, and the large part of the switching power loss is produced by the tailing current (10).

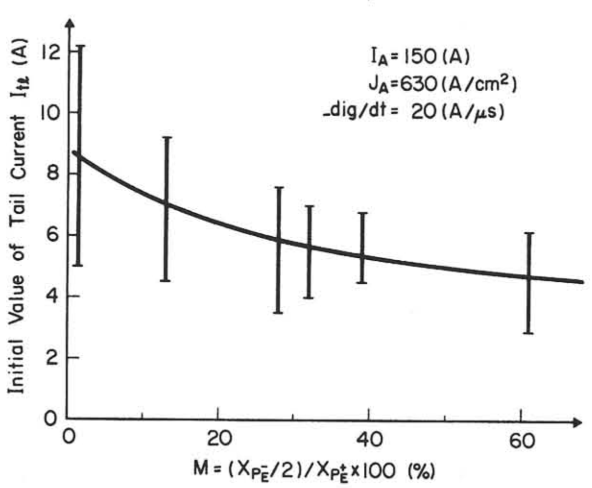

Fig.5 Tailing current vs. $(Xpe^-/2)/Xpe^+$.

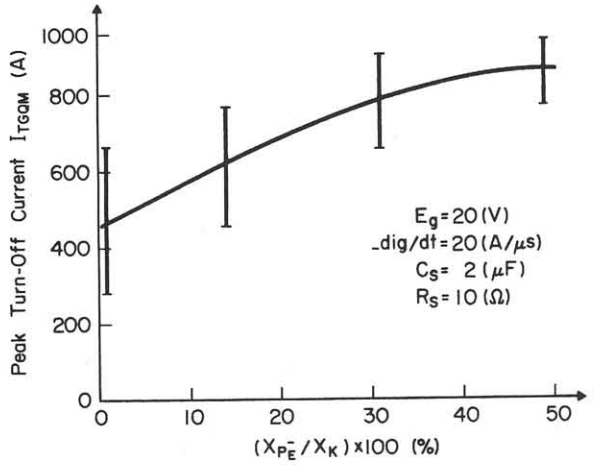

Fig.6 Peak turn-off current vs. Xpe^-/Xk.

Therefore, p^+p^--emitter GTO with large M value is promissing device in order to attain the higher frequency operation more than 1kHz.

Figure 6 shows I_{TGQM} as a function of the ratio (Xpe^-/Xk). I_{TGQM} is a monotonically increasing function of (Xpe^-/Xk). Consequently, 1.5-2.0 times of I_{TGQM} can be attained compared with the conventional RB-GTO ((Xpe^-/Xk)=0).

In contrast to these turn off characteristics, no distinctive defference can be found in the latching currents and the forward voltage drops in the range of $Xpe^-/Xk \leqq 0.5$, however, slight increases are found beyond 0.5 of Xpe^-/Xk.

From these results, we can set up the optimum design parameters of p^+p^--emitter GTO. The value of Xpe^- can be chosen from the dependences of I_{TGQM} and Vf on the parameter (Xpe^-/Xk), that is $Xpe^-=0.5Xk$. And Xpe^+ can be set up from the result of Fig.5. As is evident from this figure, the reduction rate of Itl becomes somewhat small at $(Xpe^-/2)/Xpe^+ > 0.5$. On the other hand, Xpe^+ must be as large as possible in order to maintain the good turn-on and on-state characteristics. Therefore, it is recommended that $Xpe^+=Xpe^-$.

§5. Conclusion.

The authors developed high-current, high-frequency RB-GTOs for the purpose of applications to current-mode inverters, choppers and active filters. To satisfy at the same time both characteristics of high turn-off current and high frequency, we adopted the novel anode emitter structure which consists of a horizontally alternate low-high doped layer, instead of conventional control on the n-base carrier lifetime. Optimizing the dimension of low- and high-doped regions leads to suppression of the current crowding into the central portion of the cathode emitter strip during the turn-off, as well as restriction of the extra carrier injection from the anode emitter. As a result, both of the peak turn-off current and the permissible operating frequency increased, retaining faborable turn-on and on-state characteristics.

Acknowledgment

The authors wish to thank Dr.A. Kasami and Mr.Y.Zohda for support of this work, and to thank Mr.M.Asaka for fabrication of devices.

Referrences

(1) E.D.Wolley et al., 1973 IEEE Conference Record, p.251.
(2) M.Azuma, A.Nakagawa and K.Takigami, JJAP, vol.17, pp.275-281, 1978.
(3) M.Azuma, M.Kurata and K.Takigami, IEEE Trans. Electron Devices, vol. ED-28, pp.270-274, 1981.
(4) T.Nagano, T.Yatsuo and M.Okamura, IEEE-IAS'81 Annual Meeting Rec., p.750
(5) T.Yatsuo, T.Nagano, H.Fukui, M. Okamura and S.Sakurada, 1983 IEEJ-IPEC Record, pp.65-74.
(6) T.Shinohe and M.Azuma, 1983 IEEJ-Annual Meeting Record No.450.
(7) T.Shinohe, M.Asaka and K.Takigami, 1984 IEEJ-Annual Meeting Record No.441.
(8) H.Ohashi and A.Nakagawa, 1981 IEEE-IEDM Record, pp.414-417.
(9) A.Nakagawa and D.H.Navon, IEEE Trans. Electron Devices, vol.ED-31, pp.1156-1163, 1984.
(10) T.Shinohe, K.Takigami and M.Azuma, 1983 IEEJ-IPEC Record, pp.75-86.